Interstrand Coupling Properties of LARP High Gradient Quadrupole Cables in Response to Variations in Cable Design and Heat Treatment Condition

E.W. Collings, M.D. Sumption, M. Majoros, X. Wang, D.R. Dietderich, K. Yagotyntsev, and A. Nijhuis

***Abstract*— Calorimetric measurement of coupling loss versus frequency has been measured on two sets of cored and uncored LARP high gradient quadrupole Nb_3Sn Rutherford cables. Studied are the responses of the resulting interstrand contact resistances (ICR) to variation of stainless-steel (SS) core width and position and to variation of reaction-heat-treatment (RHT) condition. One pair of cables (an early HQ-series type) with and without core had received RHT under 20 MPa uniaxial face-on pressure. Another set of cables (recent QXF type) furnished with SS cores of various widths had received RHT under ambient pressure. The results were displayed as cable-cross-sectional micrographs and plots of ICR versus percent core coverage (*W*). The HQ cables were tightly compacted and produced results consistent with a previously expected continuous ICR versus *W* variation. On the other hand the QXF cables were uncompacted such that their upper and lower layers were separated by what is referred to as a full-width "pseudocore"; as a result their ICRs were independent of the widths of the SS cores. Compaction versus noncompaction is discussed and future research directions suggested.**

***Index Terms*— Rutherford cables, Nb_3Sn cables, cored cables, interstrand contact resistance, coupling current, coupling magnetization, reaction-heat-treatment**

I. Introduction

THE HIGH luminosity upgrade [1] of the large hadron collider (LHC) at CERN will incorporate 150 mm aperture low-beta quadrupole magnets in the ATLAS (A Toroidal LHC ApparatuS) and CMS (Compact Muon Solenoid) interaction regions. For this application the US LHC Accelerator Research Program (LARP) in close collaboration with the CERN HL-LHC (High Luminosity Large Hadron Collider) project is developing a magnet designated MQXF wound with 18 mm wide 40-strand Rutherford cables [2][3]. The MQXF magnet design and the associated QXF-conductor requirements evolved from the earlier 120 mm aperture HQ-series magnets [4][5][6]. Measurements of HQ-type cables [7] and subsequently HQ magnets [4][8] demonstrated that the presence of a stainless steel core between the two layers of a Rutherford cable could increase the effective interstrand contact resistance (ICR) and by doing so suppress the interstrand coupling current (hence coupling magnetization) and reduce field distortion during current ramp. Based on these observations it was postulated that a 25 μm thick stainless steel core may be needed in the cables for the MQXF magnet. Accordingly, to further understand the impact of the core's width and location on ICR a set of QXF cables was fabricated with various core configurations. The effect of cable preparation condition was also examined.

In all of our previous studies of ICR in uncored and cored Nb_3Sn cables, conducted in collaboration with magnet groups at the Lawrence Berkeley National Laboratory (LBNL) and the Fermi National Accelerator Laboratory (FNAL) [7][9] the sample cable-stacks had been reaction-heat-treated (RHT) under 20-35 MPa face-on uniaxial pressure. This procedure was intended at the time to reproducibly represent the conditions experienced by a cable during magnet fabrication. As listed in [10] the average ICR obtained from some 12 experiments on an assortment of uncored cables after RHT under 20 MPa was 0.26 ± 0.1 μΩ; in particular an HQ-type cable produced an ICR of 0.33 μΩ [11]. The ICR of the uncored HQ cable (H1) of the present study, after RHT under 20 MPa, was also 0.33 μΩ. But to more closely represent magnet fabrication conditions the experimental cable stack, rather than being uniaxially compressed, should be "confined" to a closed channel. In the HQ magnets referred to in [4] the coils were radially confined during RHT. The confinement may have been too restrictive since measurements of ICR yielded values ranging from 0.13 μΩ to 0.4 μΩ with an average ICR of 0.25 ± 0.08 μΩ in good agreement with the 0.33 μΩ of a fully compressed cable stack.

Ideally the cable stack is confined in a closed channel just large enough to contain it during RHT when expansions of 1.5% in width and 4.5% in thickness take place. The present set of QXF cables were mounted by LBNL and heat treated in this way. It will be shown below that the resulting weakness of upper-and-lower interstrand contact had a profound effect on

Funding was provided by the U.S. Department of Energy, Office of High Energy Physics, under Grants No. DE-SC0010312 and DE-SC0011721 (OSU) and DE-AC02-05CH11231 (LBNL).

E.W. Collings, M.D. Sumption, and M. Majoros are with the Center for Superconducting and Magnetic Materials (CSMM), Dept. of Materials Science and Engineering, The Ohio State University, Columbus, OH, USA. Corresponding author e-mail: sumption.3 @osu.edu

X. Wang and D.R. Dietderich (retired) are associated with the Superconducting Magnet Group, Lawrence Berkeley National Laboratory (LBNL), University of California, Berkeley, CA, USA

K. Yagotyntsev and A. Nijhuis are with the Energy, Materials, and Systems Group, the University of Twente, Enschede, NL

the ICR.

But the strength of the contact, and the reproducibility of the ICR, will depend on the level of confinement – whether it is defined in terms of the bare reacted cable dimensions or whether it takes into account the ideal thickness or actual thickness of the insulation. The level of confinement will need to be closely defined.

II. Experimental

A. Cable Samples and Preparation for Measurement

Two coils of 35-strand HQ-type Rutherford cable and six coils of 40-strand QXF-type cable were supplied for these experiments by LBNL, Tables I and II. Cut lengths of HQ cable each enclosed in s-glass braid were loaded five-high into a special stainless steel fixture designed to apply side constraint as they were uniaxially compressed to 20.00 ± 0.01 MPa in preparation for RHT. Braid-coated lengths of QXF cable were subsequently loaded four-high into the same fixture this time configured to enable RHT at prescribed constraint. After RHT each of the cable packs was wrapped in Teflon film, placed in an aluminum mold, and bolted down: (a) under uniaxial compression of 5.01±0.00 MPa (the HQ-pair), and (b) under light pressure (the QXF set) and vacuum impregnated with CTD-101 resin. After curing the cable packs were trimmed to length in readiness for AC loss measurement.

TABLE I: Strand Details

Cable Type (Table II)	HQ	QXF
Strand source, type	OST-RRP,108/127	OST-RRP,108/127
Strand diam., d_s, mm	0.778	0.852
SC filament count	108	108
Non-Cu content, %	45.5	44.0-45.6
Strand anneal	4h/185-190°C	12h/175°C
Filament OD, d_0, μm [(a)]	51.5	62.2
Prior int.-Sn diam., d_i, μm [(a)]	28.8	30.9
Eff. fil. diam., d_{eff}, μm[(b)]	61.8	72.4

[(a)] Measured at OSU by SEM after RHT
[(b)] Calculated using $d_{eff} = d_0(1-R^3)/(1-R^2)$ with $R = d_i/d_0$[12]

B. Measurement of Cable AC Loss and Strand Magnetization

AC loss measurements are made at 4.2 K by boil-off calorimetry at the Energy, Materials, and Systems Laboratory of the University of Twente. The total AC loss per cycle, $Q_t(f) = Q_h + Q_{coup}(f)$, where Q_h is the strand's "persistent current" loss and $Q_{coup}(f)$ is the interstrand coupling loss, is generated by transverse AC fields of amplitude B_m = 400 mT and frequencies, f, of up to 60 mHz. The crossover and side-by-side (adjacent-strand) ICRs, R_c and R_a, of the cables under test were obtained by analyzing the loss versus frequency data.

III. Coupling Loss in Cables

Under LHC operating conditions field errors will be acceptably low provided the cables meet certain R_c and R_a specifications. These resistances can be extracted from the results of AC-loss measurements carried out at relatively high applied-field ramp-rates, dB/dt or frequencies, f. As explained in [13] the coupling losses per cycle per m^3 of a cable exposed to fields linearly ramping at a rate dB/dt to amplitude B_m applied perpendicular (face-on, FO) to the cable's broad face is given by:

$$Q_{coup(FO)} = \left(\frac{4}{3}\right)\left(\frac{w}{t}\right)L_p B_m \left(\frac{N^2}{20}\right)\left[\frac{1}{R_c}+\frac{20}{N^3 R_a}\right].\left(\frac{dB}{dt}\right) \text{J/m}^3 \quad (1)$$

for a cable of width w, thickness t, strand count N, and transposition pitch $2L_p$. Then after transforming dB/dt to a sinusoidal frequency, f (by way of $(dB/dt) = (\pi^2/8)4.f.B_m$, as explained in [13]) we have for the FO and edge-on (EO) losses, respectively:

$$Q_{coup(FO)}(f) = \left(\frac{\pi^2}{30}\right)\left(\frac{w}{t}\right)L_p B_m^2 N^2 \left[\frac{1}{R_{eff}}\right].f \quad (2)$$

$$Q_{coup(EO)}(f) = \frac{1}{2}\left(\frac{t}{w}\right)L_p B_m^2 \left(\frac{1}{N}\right)\left(\frac{1}{R_a}\right).f \quad (3)$$

Eqns. (1) and (2) express the FO-measured coupling loss or coupling magnetization ($M_{coup} = Q_{coup}/4B_m$, see [14]) in terms of a pair of parallel resistors R_c and $(N^3/20)R_a$ enabling an "equivalent" or "effective" R_{eff} to be defined as $1/R_{eff} = 1/R_c + 20/N^3R_a$. It is clear that R_{eff} itself is not a real cable resistance but just a ***number*** emerging from the loss experiment. As such it is a useful index of coupling magnetization, especially when cable-cores of varying widths are introduced. Thus for example R_{eff} would increase from R_c to $(N^3/20)R_a$ with increase in core coverage from 0 to 100%.

TABLE II: Cable Details [(a)]

LBNL name	(b)	HQ1020ZB	HQ1021ZB	QXF 1055z-C	QXF 1055z-K	QXF 1055z-Q	QXF 1055z-O	QXF 1055z-M	QXF 1055z-D
OSU name	**H1**	**H2**		**Q1**	**Q2**	**Q3**	**Q4**	**Q5**	**Q6**
Strand count	35	35	35	40	40	40	40	40	40
Pitch, $2L_p$, mm	98	98	98	109	109	109	109	109	109
Width, w, mm[(c)]	14.77	14.77	14.77	18.13	18.13	18.14	18.14	18.14	18.14
Av. thick, t, mm[(c)]	1.350	1.376	1.375	1.521	1.524	1.521	1.522	1.525	1.514
Keystone, deg.	0.734	0.734	0.717	0.580	0.532	0.536	0.555	0.560	0.574
pack factor, %	85.54	85.55	85.53	87.04[(d)]	86.89[(d)]	87.03[(d)]	86.98[(d)]	86.80[(d)]	87.38
Core material	No core	AISI-316L	AISI-316L	AISI-316L	AISI-316L	AISI-316L	AISI-316L	AISI-316L	No core
Core width, mm	0	8	--	11.9	15.9	15.4	14.3	13.3	0
Core cover, %[(e)]	0	60	--	72	96	93	86	80	0
Core bias	--	Major edge	--	Major edge	Major edge	Major edge	Major edge	Major edge	--

[(a)] HQ cables heat treated @ BNL: 72h/210°C + 48h/400°C+ 48h/650°C . QXF cables heat treated @ LBNL: 68h/210°C +45h/401°C+48h/650°C
[(b)] Mixture of 1020 and 1021with cores extracted
[(c)] Pre-HT values; during HT w will expand 1.5% and t will expand 4.5%
[(d)] Packing factors do not account for core volumes. For QXF cables, cores add 1.1- 1.5% to PF depending on core width
[(e)] Based on internal cable width = $w - 2d_s$ after HT

If the ICR is relatively large $Q_{coup(FO)}(f)$ is linear and R_{eff} can be obtained from its reciprocal slope, Eqn. (2). But if ICR is small it may be necessary to invoke the full frequency dependence of the coupling loss, viz.:

$$Q_{coup(FO)}(f) = \left(\frac{\pi^2}{30}\right)\left(\frac{w}{t}\right) L_p B_m^2 N^2 \left[\frac{1}{2\pi DE}\right] \cdot \frac{(f/f_c)}{1+\left(f/f_c\right)^2} \qquad (4)$$

which shows $Q(f)$ passing through a maximum at some critical frequency, f_c. This leads to two more approaches to the determination of R_{eff} : (1) from the reciprocal initial slope of the fitted $Q(f)$, and (2) from f_c since, as explained by Verweij [15], $R_{eff} = 2\pi(DE)f_c$ in which E is a function of (w/t) and the number of cables in the stack and D is a function of N and L_p.

IV. ICRS IN LHC DIPOLES AND QUADRUPOLES AND THE ROLE OF THE CORE

The use of fully insulated strands would eliminate interstrand coupling but at the expense of cable instability. So a compromise is sought; an ICR that enables adequate current sharing and acceptable coupling magnetization. Thus for LHC cables it was early on agreed that R_c should be in the range 15 ± 5μΩ [16] while R_a may be very much smaller in the interest of current sharing. An R_a as small as 0.2 μΩ was allowed [15] since its contribution to the LHC cable's R_{eff}, viz: $(N^3/20)R_a = (28^3/20)\text{x}0.2 = 220$ μΩ would not seriously degrade the combined $R_{eff} \approx R_c$.

Subsequently values of R_c much higher than 20 μΩ were obtained for LHC dipoles and quadrupoles based on: (i) rotating-coil measurements of multipole amplitudes ($<R_c>_{AV.}$ = 135 μΩ); (ii) AC loss measurements of dipoles (30 to >100 μΩ) and quadrupoles (159 to 198 μΩ); (iii) field-advance measurements of quadrupoles (95 to 230 μΩ) – see [10] for further details. Evidently such ICRs have contributed to the successful operation of the LHC and some average of them might be considered as a replacement for the above 10-20 μΩ target. But the true index of field error is not just R_{eff} but the coupling magnetization, M_{coup}, which is also proportional to the cable-design parameters (w/t), L_p, and N, Eqn.(1). So to maintain a constant M_{coup} as cable design is varied the target R_{eff} must be suitably modified. For example if R_{eff} = 100 μΩ is picked for an LHC-inner cable with (w/t), L_p, and N values of 7.49, 55 mm, and 28, respectively, then for an uncored QXF cable with corresponding design parameters 11.64, 54.5 mm, and 40 (Table II) the R_{eff} goal would be 300 μΩ.

Finally, it is important to note how M_{coup} responds to the presence of a core. Eqn.(1) indicates that $M_{coup,uncored}$ is proportional to $N^2/(20R_c)$ so a significant penalty in M_{coup} accompanies an increase in strand count. On the other hand for a full-insulating-core cable $M_{coup,cored}$ is proportional to $1/(NR_a)$. So not only is $M_{coup,cored}$ much smaller than $M_{coup,uncored}$ it decreases still further with increasing N.

V. RESULTS

The results of the total calorimetric AC loss measurements $(Q_h + Q_{coup(FO)})$ are displayed in Fig. 1. The deduced R_{eff} values and R_a values are presented in Table III. For the QXF set, Fig.1 displays both the FO and EO losses and indicates that $(dQ/df_{FO})/(dQ/df_{EO})$ >>1; predicted by Eqns. (2) and (3) that ratio is in fact about 1.8x 10^3.

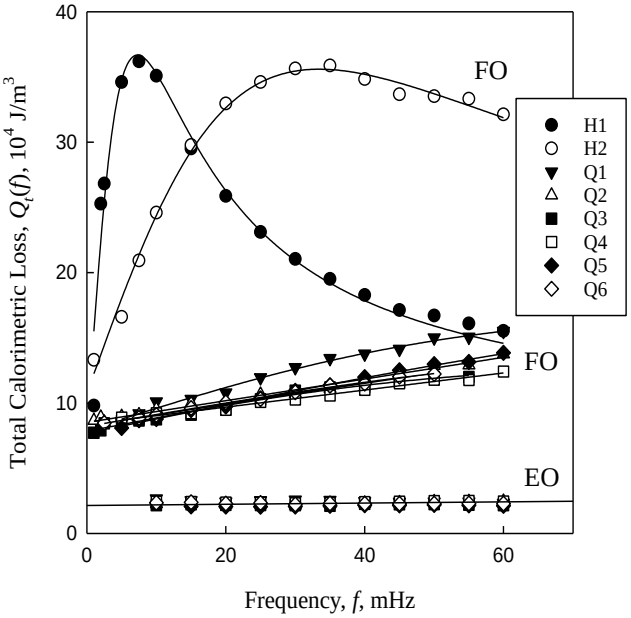

Fig. 1 Total calorimetrically measured AC loss in FO applied fields for the HQ cable pair H1 and H2 and the QXF cable set Q1-Q6. The lower group of lines depicts the EO losses for the QXF cable set

R_{eff} versus percent core coverage (W, %) for the HQ and QXF cables are plotted in Figs 2(a) and 2(b). For an ideal set of cables furnished with insulating cores of various widths the Fortran program CUDI© [17] enables coupling power, P_{coup}, to be calculated as function of W. Then using Eqn. (2) and recognizing that $P_{coup} = Q_{coup}.f$ and that for a sinusoidal wave $(dB/dt)_{AV.} = (\pi^2/8)4.f.B_m$ [13] we find

$$P_{coup} = \left(\frac{4}{30.\pi^2}\right)\left(\frac{w}{t}\right) L_p N^2 \left[\frac{1}{R_{eff}}\right] \cdot \left(\frac{dB}{dt}\right)^2 \quad \text{(W/m}^{\cdot}\text{)} \qquad (5)$$

This expression, after volume normalization and insertion of the cable parameters, enables a conversion of the CUDIE©-calculated P_{coup} to an R_{eff}. The resulting R_{eff}s for the present cables are plotted versus W as continuous lines in Fig. 2. In this model, cores of continuously increasing width are pegged (biased, see Table II) to the edges of the cables.

TABLE III: EFFECTIVE ICR AND CORRESPONDING RA VALUES*

OSU name	H1	H2	Q1	Q2	Q3	Q4	Q5	Q6
W%	0	60	71	95	94	86	80	0
R_{eff}, μΩ	0.33	2.13	27.7	63.8	66.0	81.1	52.1	65.8
R_a, nΩ			9	20	21	25	16	21

*$R_a = (20/N^3)R_{eff}$

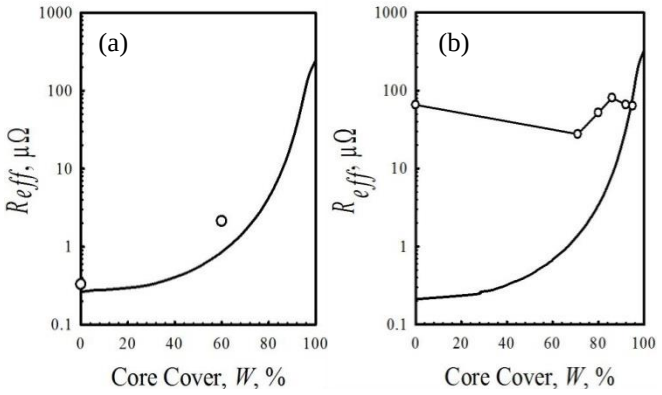

Fig. 2 R_{eff} versus W for (a) the HQ cables H1 and H2 and (b) the QXF cable set Q1-Q6. Open circles are experimental data, smooth curves are results from CUDI[(c)] models (straight lines connecting data in (b) are guides for the eye).

VI. DISCUSSION OF THE RESULTS

The coupling properties of the cables are discussed with reference to the micrographs, Fig 3. The HQ cables were bolted down in fixtures to 20 MPa at Ohio State University for RHT at Brookhaven National Laboratory. The QXF cables were constrained in fixtures at LBNL for RHT also at LBNL. In response to these two different preparation procedures: (1) the upper and lower layers of the HQ cables (both uncored and cored) became tightly pressed together, Figs. 3(a) and (b), (2) those of the QXF cables became widely separated, Figs. 3(c) and (d), and (3) the cable sets exhibited distinctly different loss behaviors, Fig. 1.

The HQ Cables H1 and H2: We first of all note the reproducibility of the uncored HQ data. Measurement of the compacted HQ cable H1 yielded an average R_c of 0.33μΩ as did the previous measurement of a compacted HQ-type cable [11]. The insertion of a partial-width core (W = 60%) raised R_{eff} to 2.1 μΩ and following the results of CUDI© analysis, Fig. 2(a), we expect R_{eff} to increase continuously to some usefully high value as W increases into the high 80s or 90s.

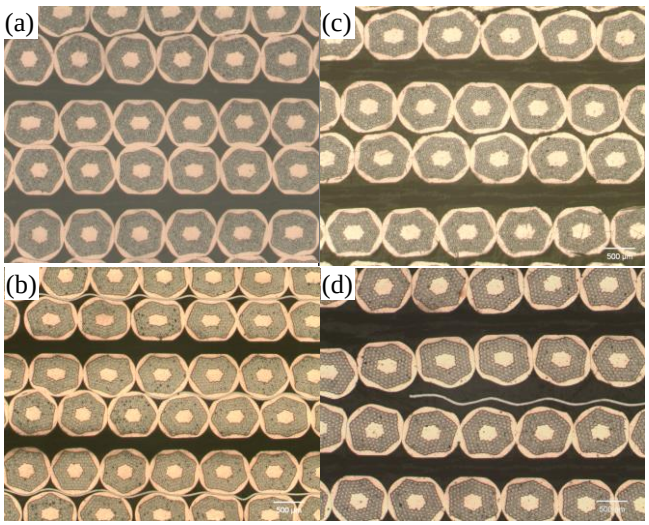

Fig. 3. (a) uncored H1 and (b) cored H2; (c) uncored Q6 and (d) cored Q5 (representative of the entire cored QXF set).

The QXF Cables Q1-Q6: Fig. 3(c) shows lack of contact between the upper and lower strand layers and Fig. 3(d) shows the stainless-steel (SS) core floating in the space between the layers. The gap between the layers is equivalent to a full-width insulating core. Such an "epoxy pseudocore" is present in all the QXF cables, the SS core itself playing no role. As noted above, sample preparation conditions were chosen to more closely mimic those of actual magnet fabrication. However, it seems that "zero compaction but constraint only" can lead to cable conditions which are not well defined and may allow for gaps. The accompanying "W-independent" R_{eff} is shown in Fig. 2(b) to intersect the CUDI© prediction at W = 91-95%. With this level of coverage it follows that R_{eff} depends predominantly on the adjacent-strand contact

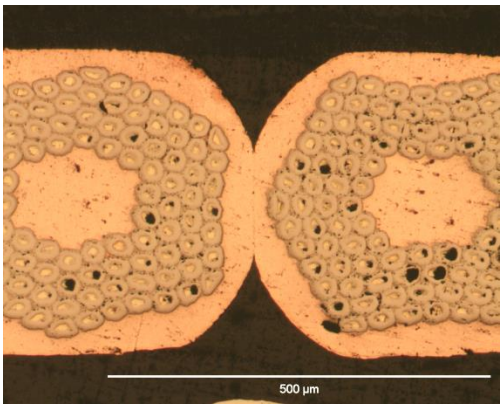

Fig. 4. Well-bonded adjacent-strand contact in a QXF cable.

resistance R_a, in which case $R_a = (20/N^3)R_{eff}$. Following this prescription R_a values of 9-25 nΩ are obtained, Table III, consistent with the tight adjacent-strand contact noted in enlarged versions of Figs. 3(c) and (d), e.g. Fig.4.

VII. CONCLUSIONS

To obtain usefully high R_{eff}s for compacted cored cables coverage values of 80-90% are required. But as summarized in [10] for any given W in that range a considerable scatter in R_{eff} can be expected depending on the type, width, and placement of the core. For a fixed set of such parameters the reproducibility of R_{eff} has not been explored or quantified; a core may be useful in moderating any such variations in practice. A full-width "epoxy pseudocore" is present in all the noncompacted QXF cables. For these, R_{eff} depends predominantly on R_a. Future studies might investigate how the R_a of another group of the same cables, ostensibly prepared in the same way, would respond to what might turn out to be a different set of side constraints. Similarly, it would be useful to explore the level of local compaction in cables in different parts of an accelerator magnet prepared under a given constraint. Finally, explorations of ICR vs "level of constraint" are needed.

ACKNOWLEDGMENTS

Cables were wound by H. Higley; RHT at BNL and LBNL.

REFERENCES

[1] L. Bottura, G. de Rijk, L. Rossi, and E. Todesco, "Advanced accelerator magnets for upgrading the LHC", *IEEE Trans. Appl. Supercond.* **22** 4002008 (2012)

[2] A. Ghosh, "QXF conductor and cable" *DOE Review of LARP*, Feb. 17-18 (2014)

[3] G. Ambrosio, "Nb_3Sn high field magnets for the high luminosity LHC upgrade project", *IEEE Trans. Appl. Supercond.* **25** 4002107 (2015)

[4] X. Wang, G. Ambrosio, F. Borgnolutti, M. Buehler, et al., "Multipoles induced by inter-strand coupling currents in LARP Nb_3Sn quadrupoles", *IEEE Trans. Appl. Supercond.* **24** 4002607 (2014)

[5] G. Chlachidze, G. Ambrosio, M. Anerella, F. Borgnolutti, et al., "Performance of HQ02, an optimized version of the 120 mm Nb_3Sn LARP quadrupole", *IEEE Trans. Appl. Supercond.* **24** 4003805 (2014)

[6] P. Ferracin, " From LARP HQ to MQXF strand, cable and coil" and "From LARP HQ to MQXF magnet design" in MQXF Design and Conductor Requirements, *MQXF Conductor Review*, CERN November 5-6 (2014)

[7] E.W. Collings, M.D. Sumption, M.A. Susner, D. Dietderich, E. Kroopshoop, and A. Nijhuis, "Interstrand contact resistance and magnetization of Rutherford cables with cores of different materials and widths", *IEEE Trans. Appl. Supercond.* **22** 600904 (2012)

[8] J. DiMarco, G. Ambrosio, M. Buehler, G. Chlachidze, et al., "Field quality measurements of LARP Nb_3Sn magnet HQ02", *IEEE Trans. Appl. Supercond.* **24** 4003905 (2014)

[9] E.W. Collings, M.D. Sumption, E. Barzi, D. Turrioni, R. Yamada, A.V. Zlobin, Y. Ilyin, and A. Nijhuis, "Magnetic measurements of AC loss in cored Nb_3Sn Rutherford cables – interstrand contact resistance as function of core width", *Adv. Cryo. Eng. (Materials)* **54** 285-292 (2008)

[10] E.W. Collings, M.D. Sumption, M. Majoros, X. Wang, et al., "Effects of core type, placement, and width, on the estimated interstrand coupling properties of QXF-type Nb_3Sn Rutherford cables", *IEEE Trans. Appl. Supercond.* **25** 4802805 (2015)

[11] E. W. Collings, M. D. Sumption, M. A. Susner, D. R. Dietderich, and A. Nijhuis, "Coupling loss, interstrand contact resistance, and magnetization of Nb_3Sn Rutherford cables with cores of MgO tape and s-Glass Ribbon", *IEEE Trans. Appl. Supercond.* **21** 2367-2371 (2011)

[12] M.D. Sumption, X. Peng, E. Lee, X. Wu, and E.W. Collings, "Analysis of magnetization, AC loss, and d_{eff} for various internal-Sn based Nb_3Sn multifilamentary strands with and without subelement splitting", *Cryogenics* **44** 711-725 (2004)

[13] M.D. Sumption, E.W. Collings, R.M. Scanlan, A. Nijhuis, and H.H.J. ten Kate, "Core suppressed AC loss and strand-moderated contact resistance in a Nb_3Sn Rutherford cable", *Cryogenics* **39** 1-12 (1999)

[14] E.W. Collings, M.A. Susner, M.D. Sumption, and D.R. Dietderich, "Extracted strand magnetizations for an HQ type Nb_3Sn Rutherford cable and estimation of transport corrections at operation and injection field", *IEEE Trans. Appl. Supercond.* **24** 4802605 (2014)

[15] A.P Verweij, "Electrodynamics of Superconducting cables in accelerator magnets" *Ph.D. Thesis*, University of Twente Press, 1995

[16] Z. Ang, I. Bejar, L. Bottura, D. Richter, M. Sheehan, et al., "Measurements of AC loss and magnetic field during ramps in the LHC model dipoles", *IEEE Trans. Appl. Supercond.* **9** 735-741 (1999)

[17] A.P. Verweij, "CUDI: a model for calculation of the electrodynamic and thermal behavior of superconducting Rutherford cables", CUDI software, © CERN